Wind and Structures, *Vol. 28, No. 4 (2019) 203-213*
DOI: https://doi.org/10.12989/was.2019.28.4.203

Aerodynamic effects of subgrade-tunnel transition on high-speed railway by wind tunnel tests

Jingyu Zhang[a], Mingjin Zhang*, Yongle Li[b] and Chen Fang[c]

Department of Bridge Engineering, Southwest Jiaotong University, Chengdu, Sichuan 610031, China

(Received March 6, 2018, Revised September 20, 2018, Accepted October 13, 2018)

Abstract. The topography and geomorphology are complex and changeable in western China, so the railway transition section is common. To investigate the aerodynamic effect of the subgrade-tunnel transition section, including a cutting-tunnel transition section, an embankment-tunnel transition section and two typical scenarios for rail infrastructures, is selected as research objects. In this paper, models of standard cutting, embankment and CRH2 high-speed train with the scale of 1:20 were established in wind tunnel tests. The wind speed profiles above the railway and the aerodynamic forces of the vehicles at different positions along the railway were measured by using Cobra probe and dynamometric balance respectively. The test results show: The influence range of cutting-tunnel transition section is larger than that of the embankment-tunnel transition section, and the maximum impact height exceeds 320mm (corresponding to 6.4m in full scale). The wind speed profile at the railway junction is greatly affected by the tunnel. Under the condition of the double track, the side force coefficient on the leeward side is negative. For embankment-tunnel transition section, the lift force coefficient of the vehicle is positive which is unsafe for operation when the vehicle is at the railway line junction.

Keywords: high-speed railway; embankment-tunnel transition section; cutting-tunnel transition section; wind tunnel test; vehicle aerodynamic coefficient; wind speed profile

1. Introduction

In western China, the complex and changeable terrain leads to various forms of the railway lines. Previous studies have shown that the forms of the cross-section of the railway not only change the wind environment above the railway but also affect the aerodynamic characteristics of the vehicles (Suzuki *et al*. 2003, Avila-Sanchez *et al*. 2014). While in a certain condition of a strong crosswind, the safety of train operation can be even threatened (Raghunathan *et al*. 2002, Chen and Cai 2004, Diedrichs *et al*. 2007, Baker *et al*. 2009). In Japan, strong winds have caused multiple train accidents (Kwon *et al.* 2010). The trains were blown over by strong winds while running from bridge to ground, and this accident caused 6 people injured and 6 people dead (Fujii *et al*. 1999). In China, strong winds have caused train outage more than 100 times, blowing over more than 100 carriages on the line between Lanzhou and Urumqi (Xiong *et al*. 2006, Ge and Jiang 2009).

In recent years, different forms of railways are selected as study objects and investigated, and wind tunnel tests and numerical simulation are the two most common research methods (He *et al*. 2014, Dorigatti *et al*. 2015, Giappino *et al*. 2016, Alonso-Estébanez *et al*. 2018). Taking long span bridge as the study object, some researchers analyzed the dynamic responses of bridges and vehicles under crosswind (Xu *et al*. 2003, Xia *et al*. 2008, Li *et al*. 2013). The embankment, a typical scenario for railway, can affect the wind environment above the tracks and cause safety risks (Quinn *et al*. 1998, Hu and Pan 2010, Tomasini *et al*. 2014). Baker (1985) explored the effect of topography on the wind speed above the embankment by means of wind tunnel tests and field measurements. Baker *et al.* (2004) also compared the wind forces on trains under full-scale tests and wind tunnel tests and found that there is a reasonably good agreement in side force and moments. Suzuki *et al* (2003)studied the impacts of embankment parameters on vehicle aerodynamic characteristics, and the wind profiles above the embankment were obtained as well. Focusing on the embankment, the following conclusions can be obtained by wind tunnel tests (Cheli *et al*. 2010, Cheli *et al*. 2013):

- The overturning moment of the vehicle is related to wind speed;
- With the vertical force, lateral force and overturning moment as criterions, the aerodynamic load of the vehicle increases with the enlargement t of turbulence integral scale.

Besides, the effect of Reynolds number on the vehicle was also investigated (Bocciolone *et al*. 2008, Tomasini *et al*. 2014). Using the numerical simulation method, the effects of different cutting parameters, such as the depth and slope gradient of the cutting, on vehicle aerodynamics had been studied (Zhang *et al*. 2015). Through computational fluid dynamics (CFD) method, Liu *et al* (2018) approached the vehicle aerodynamic characteristics while the vehicle

*Corresponding author, Lecturer
E-mail: zhang-Minjin@swjtu.edu.cn
[a] Ph.D. Candidate
E-mail: zhangjycd@live.com
[b] Professor
E-mail: lele@swjtu.edu.cn
[c] Ph.D. Candidate
E-mail: fangchenwave@163.com

ISSN: 1226-6116 (Print), 1598-6225 (Online)

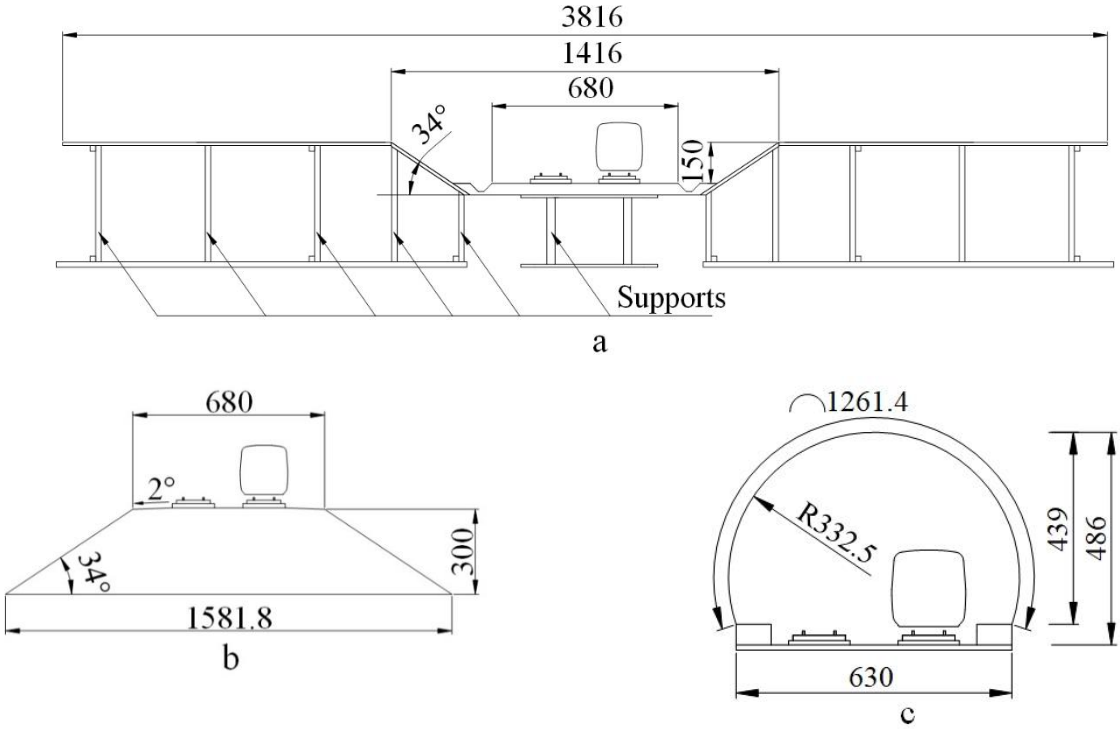

Fig. 1. Testes configuration of each monomer model (Unit: mm): (a) 150 mm deep shallow cutting (corresponding to 3 m deep in full scale), (b) 300 mm high embankment (corresponding to 6m high in full scale), (c) tunnel with radius 332.5 mm (corresponding to 6.65 m in radius in full scale)

passing the windbreak transition section.

Among the aforementioned studies, there is still little research on the railway transition section. In the western mountain area of China, it is inevitable to excavate and fill the subgrade and dig the tunnel in the mountains, therefore, embankment, cutting, and tunnel are three typical railway forms. The raised shape of the embankment can compress the flow and accelerate the flow speed, which will change the wind environment and enhance the vehicle aerodynamic force (Schober *et al*. 2010, Tomasini *et al*. 2014). The concave shape of the cutting has an opposite effect; the shape will slow down the flow speed above the railway. As for the tunnel, the portal has a diffusion effect on flow. Thus, it is difficult to determine the vehicle aerodynamics and wind characteristics above the railway of the transition section due to the less study of subgrade-tunnel transition section. In this paper, taking an embankment-tunnel transition section, a cutting-tunnel transition section and China CRH2 trains as test objects, and in order to reduce Reynold number effect, big scale (model scale is 1:20) wind tunnel test models were established. In the tests, wind environments on different lateral positions at the railway junction and on the centerline of the railway are investigated. Meanwhile, aerodynamic forces of vehicles at different lateral positions at the railway junction and different positions along the railway are also measured.

2. Experiment setup

Tests had been performed with scale model of the CRH2 vehicle, with two different scenarios:

- 1:20 scale model for the tests on cutting-tunnel transition section (CTTS);
- 1:20 scale model for the tests on embankment-tunnel transition section (ETTS).

Wind tunnel tests were carried out in XNJD-3 wind tunnel in Southwest Jiaotong University. It is a closed-circuit atmospheric boundary layer wind tunnel with the size of 22.5 m wide, 4.5 m high and 36.0 m long. Its wind speed ranges from 1.0 to 16.5 m/s, the turbulence intensity of the free-stream flow I_x is less than 1.5% overall and the thickness of the boundary of the wind tunnel is less than 0.2m. All the tests have been undertaken with smooth flow, and neither the wind direction nor the wind attack angle was considered.

2.1 Test models

All the models are based on standard cross section drawings according to the Code for Design of High Speed Railway (TB 10621-2014 2014). Each monomer model is shown in Fig. 1. There are two tracks on the three scaled models, the separation between two tracks is 250 mm, corresponding to 5 m in full scale. As Fig. 1(a) shown, a cutting model based on 3 m deep shallow cutting was used in tests because the top of the vehicle is exposed outside the cutting, which is detrimental to vehicle stability. In the tests, the dimension is 150 mm (depth) × 680 mm (bottom width) × 6000 mm (length). To ensure the top elevation of the track of different models and reduce the blockage ratio, as the figure shown, the model was lifted by the supports, and the lateral plates at the windward side and leeward side were used to simulate the ground. The embankment model is based on a 6 m high standard embankment, and the model dimensions are as follows (see Fig. 1(b)): 300 mm high, 680mm wide at the top, 1581.8 mm wide at the bottom, and the total length is 6000 mm. The tunnel model is shown in Fig. 1(c), for the same reason as cutting model, the tunnel model was also lifted by the supports. The models placed in the wind tunnel are shown in Fig. 2. For vehicle models, the models are based on the CRH2 train, and the vehicle model is made up of three vehicles: head vehicle, intermediate vehicle (test vehicle) and tail vehicle. The dimension of the head and the tail vehicle is 1200 mm long, 169 mm wide and 175 mm high, while the intermediate vehicle is 800 mm long, 169 mm wide and 175 mm high. The head and tail vehicles, which equivalent to the pneumatic transition section, are used to ensure the stability of the intermediate vehicle and weaken the influence of the flow around the vehicle. A shorter intermediate vehicle is to reduce the influence of vibration on measurement accuracy. The maximum blockage ratio caused by the models is 4.3%, thus its effects are neglected in the next discussions.

2.2 Data measurement setup and processing

To measure the wind speed profile, a Cobra Probe with velocity typically accuracy of 0.3 m/s was used to measure the wind speed at different horizontal, vertical and longitudinal positions above the railway line. For each measurement, the sampling time lasts 45s with the sampling frequency of 256Hz.

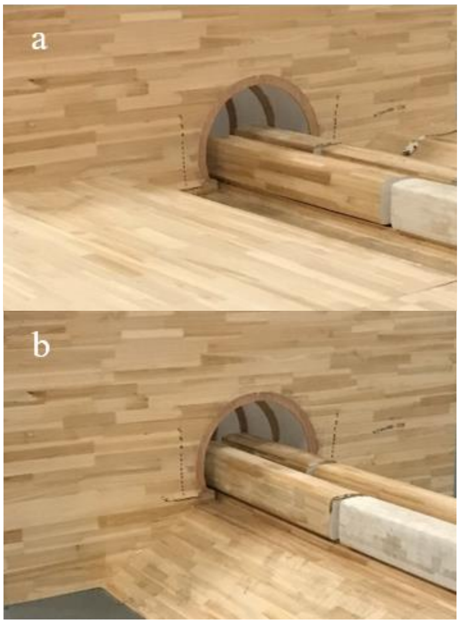

Fig. 2 Vehicles on (a) cutting-tunnel transition section, and (b) embankment-tunnel transition section

(a) Cobra wind speed instruments

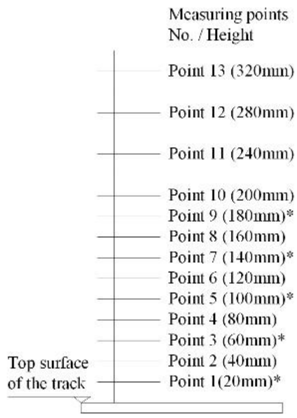

(b) The height of measuring points

Fig. 3 Cobra wind speed instruments and the height of measuring points

Also, the tests were repeated 3 times to reduce the uncertainty. The installation sketch map and the measuring points on height distribution are shown in Fig. 3, the asterisk is used to distinguish different measuring positions, and the details are shown in Fig. 6.

A 5-components dynamometric balance whose range is 5 kg and accuracy is 0.5% was installed on the intermediate vehicle to measure the vehicle aerodynamic forces. The sampling time and the sampling frequency are set to 50s and 400Hz respectively. And the final data is obtained by averaging all the collected data. As Fig. 4 shown, the balance relates to the vehicle by 4 screws, the vehicle is suspended in the balance.

Aerodynamic coefficients, including side force coefficient C_H, lift force coefficient C_V, and overturning moment coefficient C_M, are a set of non-dimension quantities describing the static wind force. The formulas can be obtained by following equations

$$C_H = F_H/(0.5\rho U^2 HL) \tag{1}$$

$$C_V = F_V/(0.5\rho U^2 BL) \tag{2}$$

$$C_M = M_Z/(0.5\rho U^2 B^2 L) \tag{3}$$

Table1 Description of test cases (refer to Fig. 6)

Test category	Test instrument	Vehicle arrangement	Position of test instrument	Case / Point number	Notes
Wind speed profile tests	Cobra Probe		Windward side Leeward side Railway centerline	RJ-WW RJ-LW RJ-CT, CU80/EM80, CU300/EM300	
Vehicle aerodynamic forces test	Dynamic balance	Single track	Windward side	1 ~ 5	Without interference vehicle
			Leeward side	6 ~ 10	
		Double track	Windward side	11 ~ 15	With interference vehicle on windward side or leeward side

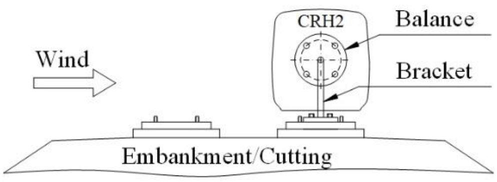

Fig. 4 Aerodynamic forces test of CRH2 vehicles

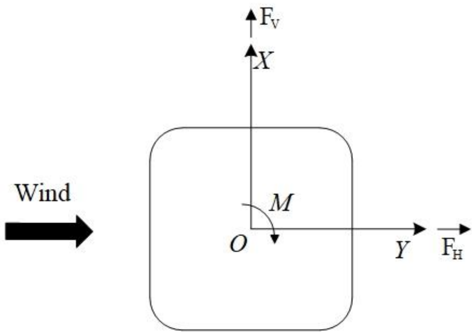

Fig. 5 Definition of aerodynamic forces

Where, F_H, F_V and M_Z are the side force, lift force, and overturning moment respectively, H, B, and L are the height, width and length of the intermediate vehicle respectively. The definitions of the coordinate system and the direction of aerodynamic forces are shown in Fig. 5.

The cases schematic is shown in Fig. 6. The wind speed at different heights at 6 positions, which are expressed by blue and red points, was tested. In the tests, the free incoming mean wind speed $U_0=10m/s$. For vehicle dynamic forces tests, the vertical dash-dot lines mean the force measuring points with adjacent measuring point spacing 200 mm, and the hollow arrow on the right side of the head vehicle is utilized to indicate the direction of the vehicle movement. For force test cases, two kinds of arrangements were investigated: (1) single track on the windward side (cases 1 ~ 5) or on the leeward side (cases 6 ~ 10), with the separation distance of 200 mm along the railway for each case, (2) double track on the railway (cases 11 ~ 20), which could take shadowing effect into consideration on windward or leeward side of the vehicle. In the tests, three different wind speeds (6 m/s, 8 m/s, 10 m/s) are considered. The case description and arrangements of both two kinds of tests are listed in Table 1.

3. Results

3.1 Cutting-tunnel transition section

3.1.1 Wind speed profiles

For railway line junction, the wind speed profiles above the windward track, leeward track and the centerline of the railway are measured. Wind speed profiles at different horizontal positions at the junction of the railway line are shown in Fig. 7. In this figure, taking the elevation of the track top surface as datum elevation and the upward direction as right direction, setting the measuring point height H as the vertical axis, while the ratio of measuring point wind speed to incoming mean wind speed U/U_0 as the horizontal axis. At railway junction, the wind speed at different horizontal positions, including centerline of the track (CTTS-CT), centerline of the windward rail track

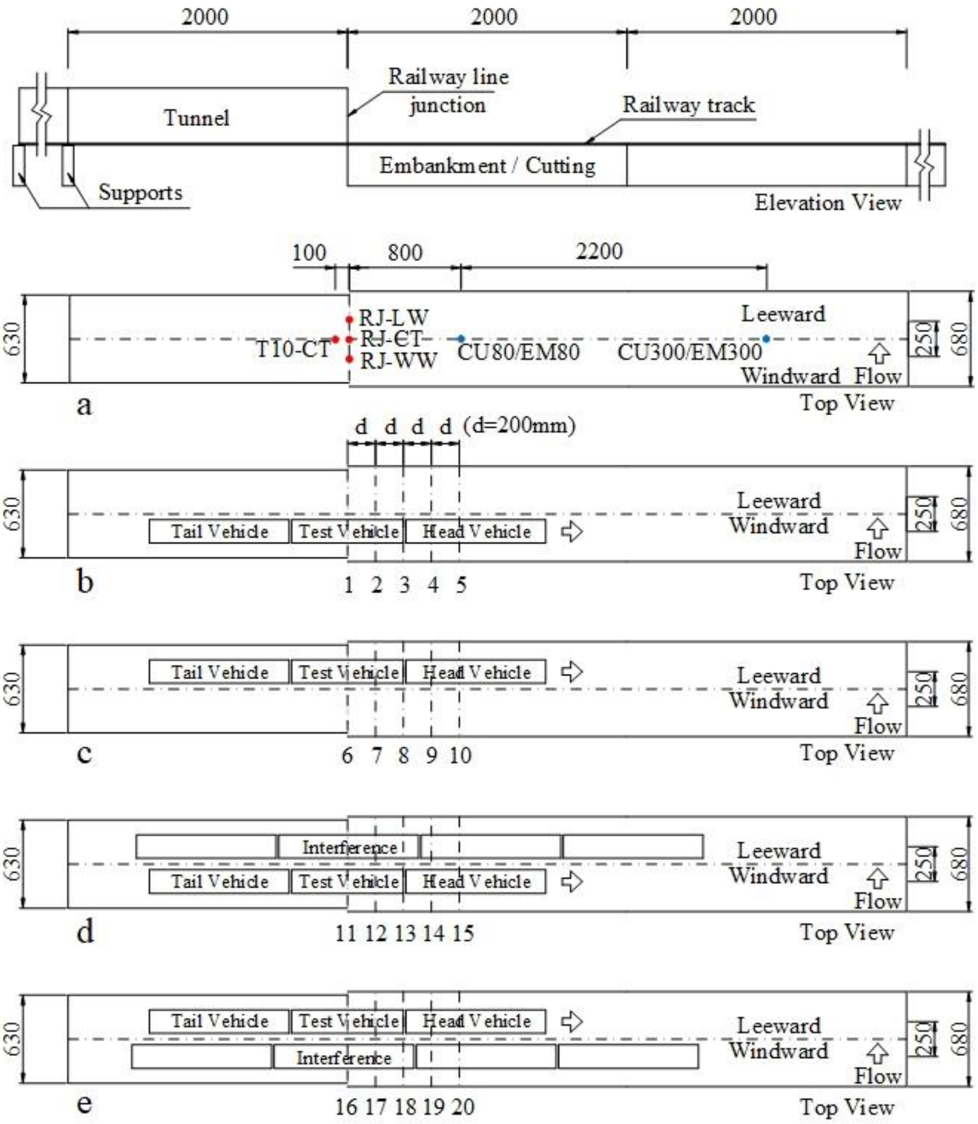

Fig. 6 The arrangements of test cases (Unit: mm): (a) the measuring position arrangements of Cobra Probe, refer Fig. 3(b), the red measuring positions contain all the points, the blues do not contain the points with symbol asterisk, (b)- (e) vehicle aerodynamic forces tests

(CTTS-WW) and centerline of the leeward rail track (CTTS-LW), above the railway increases with the measuring point height increases, but it is always smaller than the incoming mean wind speed. The variation of wind speeds on CTTS-WW and CTTS-LW are more consistent, that is, the wind speed increases with some fluctuation along the height. The variation of wind speed on CTTS-CT is the same as that on CTTS-WW and CTTS-LW, but with less fluctuation. Moreover, when the measuring point height is higher than 150 mm, the wind speed is larger than that on CTTS-WW and CTTS-LW. The outer contour of the tunnel portal has a strong diffusion of the air flow, which causes the difference of wind speed among CTTS-WW, CTTS-LW, and CTTS-CT. Comparing wind speed curve of windward side and of leeward side, it can be seen that the wind speed suddenly increases at the height of 40 mm, which may be caused by the raised unballasted track plate above the railway that produces a local compression of the air flow. From the data shown in Fig. 8, the change law of wind speed at the railway junction is the same as that above the cutting (Curve CU80 and CU300), which means that the variation of wind speed in height is dominated by cutting. When the air flows through the tunnel portal, a part of flow will be dispersed. Combining Figs. 7 and 8, it can be found that the wind speeds at positions where away from railway junction are larger than that at railway junction and closer to incoming wind speed at 320 mm high measuring points. Due to this, the shadowing effect of the slope at windward reduces the wind speed at the measuring points away from railway junction. In addition, the joint action of the shadowing effect of cutting and the space expansion effect of the tunnel portal leads to further decrease of the wind speed at the railway junction.

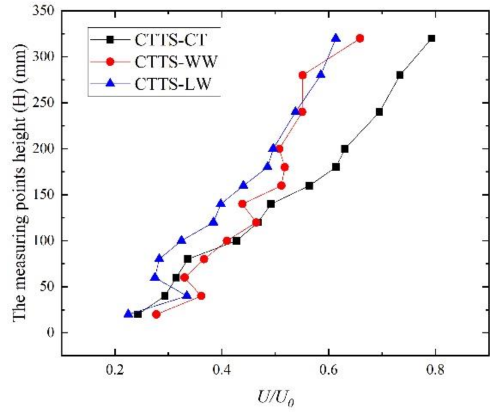

Fig. 7 Wind speed profile above the railway line at the juncture of different track

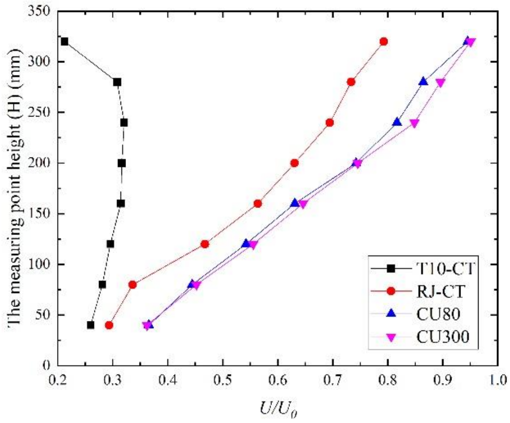

Fig. 8 Wind speed profile above the railway central line at different locations along the track

3.1.2 Vehicle aerodynamic coefficient

(1) Single train

To investigate the aerodynamic characteristics of the vehicle, the vehicle wind static forces at different positions along the railway under different wind speeds (6 m/s, 8 m/s, 10 m/s) were measured. The measuring point arrangements are shown in Fig. 6. The aerodynamic coefficients are shown in Fig. 9, the solid line indicates that the vehicle is on the windward rail track, and the dotted line means leeward rail track. From the results shown in Fig. 9, the change rule of vehicle aerodynamic coefficients with wind speed is essentially identical, but the values are changing. In full scale situation, the Reynold number Re=7.1×10^6 (Wind speed $U=30$ m/s, the vehicle height $H_V=3.5$ m), while in wind tunnel test, the Reynold number Re=0.71×10^5~1.18×10^5 (In the test, the vehicle height $h_V=0.175$ m), thus, the Reynold number in tunnel test is much less than the actual situation (Suzuki *et al*. 2003), so the Reynold number would cause the variation of aerodynamic coefficients with wind speed. For side force coefficient C_H, the change laws are almost the same along the infrastructure for both windward and leeward rail tracks. Comparing two tracks, the vehicle suffers greater side force on the leeward side, which has a good agreement with numerical simulation (Zhang *et al*. 2015).

After the vehicle completely moves out of the tunnel (cases 3 ~ 5 on windward side and cases 8 ~ 10 on leeward side), the difference of side force between two tracks becomes larger. This observation may be explained that the windward slope of the cutting makes the main direction of air flow above the windward side track inclined downward, and the bottom makes the flow horizontal at the leeward side, where the horizontal component of the flow is larger on the leeward side. Moreover, when the vehicle completely moves out of the tunnel, the windward area of the vehicle increases and enlarges the difference of C_V between two sides. For lift force coefficient C_V, the coefficient keeps negative under all conditions, and that means the vehicle is always in a safe state. Comparing two tracks, the vehicle on the leeward side is safer, and the coefficient fluctuates greatly, with a maximum of about 50%. As Fig. 9(c) shown, the fluctuation of the C_M is getting larger. It is harmful to the leeward side train for greater C_M at the railway junction, but more unfavorable to windward side train for greater fluctuation and value along the railway.

(2) Interference between two trains

For double rail track, the intersection of double trains is frequent, and the shadowing effect will be produced on the windward side or leeward side of the vehicle while the train

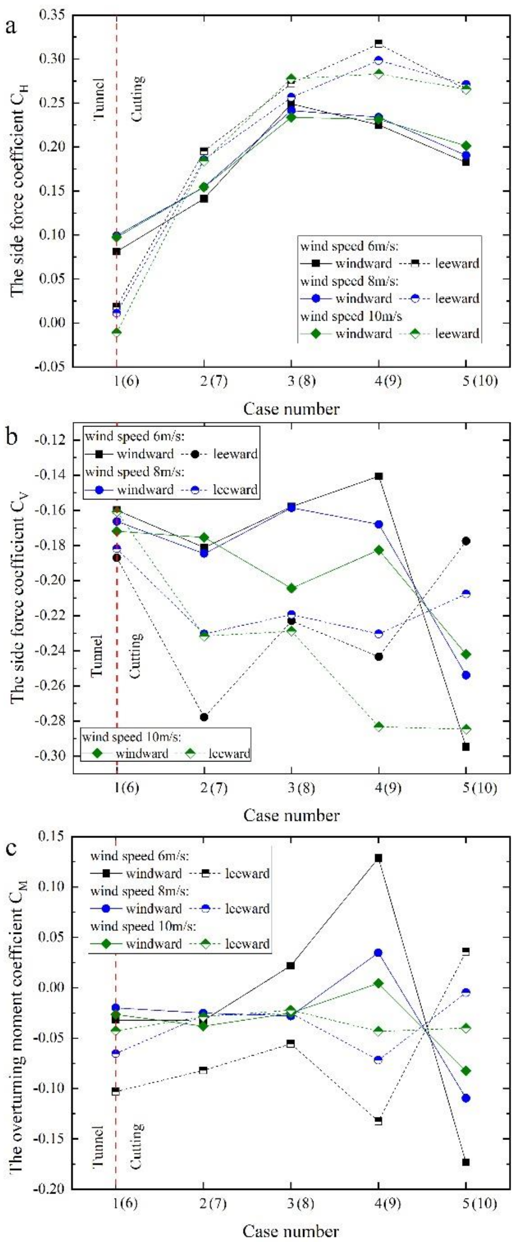

Fig. 9 Aerodynamic force coefficients at different positions along railway under the condition of single track

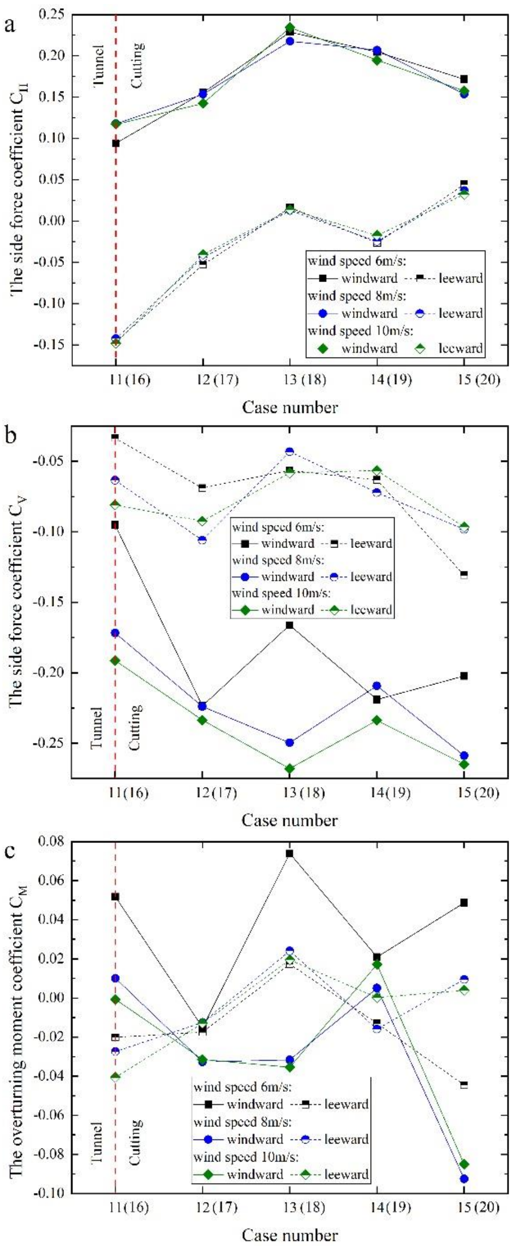

Fig. 10 Aerodynamic force coefficients at different positions along railway under the condition of double track

intersection occurs. The research object of this paper is intermediate vehicle, the influence of the aerodynamic interference produced by head/tail vehicle on intermediate vehicle is limited when two trains crossing, therefore, the method of stationary vehicle was carried out in the tests. To investigate the shadow effect on intermediate vehicle, the vehicle aerodynamic force at different positions along the line under different wind speed (6 m/s, 8 m/s, 10 m/s) were measured (the results are shown in Fig. 10). The change rule of vehicle aerodynamic coefficients with wind speed is still essentially identical, but the values are changing.

Shown as Fig. 10, because the windward side vehicle has a significant shadowing effect on the leeward side, the C_H on the windward side is greater. When the windward side vehicle moves into the tunnel, the C_H increases first and then decreases, and the maximum value appears in case 13 / case 18. For this observation, the C_H increases because the vehicle windward area increases gradually and reaches the maximum value in case 13 / 18. As the vehicle position changing, the influence of the transition section decreases, so the coefficient decreases thereafter. When the vehicle is on the leeward side, the C_H is negative first and then fluctuates near zero. This is because a negative pressure zone between two tracks is created. After the vehicle completely moves out the tunnel, the C_H of the vehicle on the leeward side also fluctuates near zero, which indicated that the vehicle is essentially not affected by the wind. In a word, considering interference between two trains, the vehicle is relatively dangerous when the vehicle on the leeward side does not fully move out the tunnel for the combined action of cutting and tunnel; the side force is very small and the vehicle is under safe for the shelter effect of cutting and windward vehicle after the vehicle moves out the tunnel.

The C_V keeps negative, which indicates that the airflow provides additional downforce, which is beneficial to the vehicle operation, on the vehicle. Overall, the directions of the C_M on the windward and leeward sides are opposite. As Zhang *et al* (2015) described, the shadow cutting is much more disadvantageous on aerodynamics, and the different simulation method and model parameters lead to the differences in the results. This circumstance could be ascribed to the fact that a vortex is formed in a region in the middle of the two trains, and the flow speed of the vortex is lower than nearby. According to Bernoulli's theorem, the relatively low-speed vortex produces thrust on the top of the train and leads to the force in the opposite direction.

3.2 Embankment-tunnel transition section

3.2.1 Wind speed profiles

All the test configurations are consistent with CTTS tests. In this part, the wind speed at different horizontal positions, including the centerline of the track (ETTS-CT), centerline on the windward side (ETTS-WW) and centerline on the leeward side (ETTS-LW), above the railway were also tested. As Fig. 11 shown, at the railway junction, the steady inflow velocity above the railway is slightly larger than the incoming flow, this phenomenon indicates that the influence height of the transition section is within the height of measuring points in the test. Comparing the wind speed profiles at different positions, we can find the following change laws: for the measuring points on the ETTS-WW and ETTS-CT, the wind speed decreases first, then increases and then tends to be stable, reaching the minimum at the height of 40 mm. When the height is higher than 240 mm, the wind speed tends to be stable and is larger than the incoming wind speed. According to the above-mentioned, when the height of the measuring point is less than 80 mm, the variations of wind speed at different lateral positions of the railway are different, which are caused by the ancillary structure above the railway. When measuring point height is higher than 100 mm, the wind speed variation at different position of the centerline is generally the same, and the wind speed on ETTS-CT is larger than that on ETTS-WW and ETTS-LW because of the side slope of the embankment. Fig. 12 shows the wind speed profile above the railway centerline along the railway. From the results, it can be found that the wind speed at the railway junction is affected by embankment and tunnel while the measuring point height is less than 240 mm. However, with the height increases, the influence of the tunnel on wind speed reduces because of the decrease of the tunnel portal lateral dimension. While the height is higher than 240 mm, the wind speed of the railway centerline is basically the same as other position (i.e., EM80, EM300), and the value is larger than incoming flow speed. Therefore, the wind speed is mainly dominated by the embankment, and the compressed flow accelerates the wind speed.

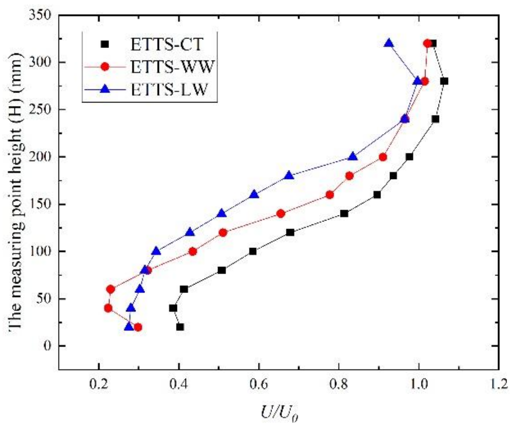

Fig. 11 Wind speed profile above the railway line at the juncture of different routes

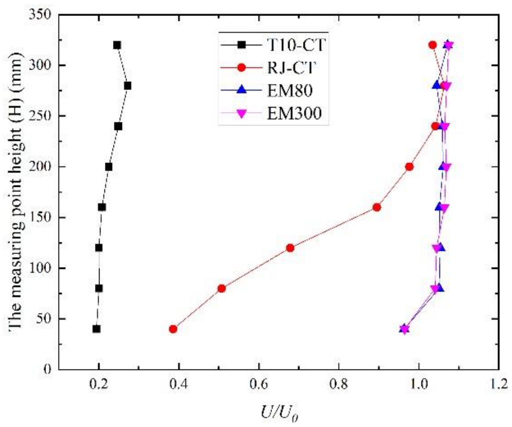

Fig. 12 Wind speed profile above the railway central line at different locations along the track

3.2.2 Vehicle aerodynamic coefficient

<u>(1) Single train</u>

The cases are set as CTTS tests, the results are shown in Fig. 13. It is consistent with the test results of vehicle aerodynamics in CTTS tests, the effect Reynold number causes the aerodynamic coefficient changing with the wind speed. According to the previous achievement, the wind speed would affect the aerodynamics indeed, and it seems that the aerodynamic forces are smaller when the wind speed is small (Tomasini *et al*. 2014). For C_H, the coefficient increases first and then tend to be stable, and the force vehicle suffered on the windward side is larger than that on the leeward side. Embankment slope not only changes the airflow direction, but also has diffusion effect on it, so when the flow passing through the embankment, the diffusion effect will be aggravated and the vertical force acting on the windward side of the vehicle will be reduced with the airflow flows. Therefore, the side force that vehicle suffered on the windward side is larger. After the vehicle moving out of the tunnel, the windward area of the vehicle remains unchanged, so the side force does not fluctuate substantially and tends to be stable while the vehicle locates at the positions of cases 3 ~ 5 / cases8 ~ 10. For C_V, it decreases first and then tends stabilized. It should be noted

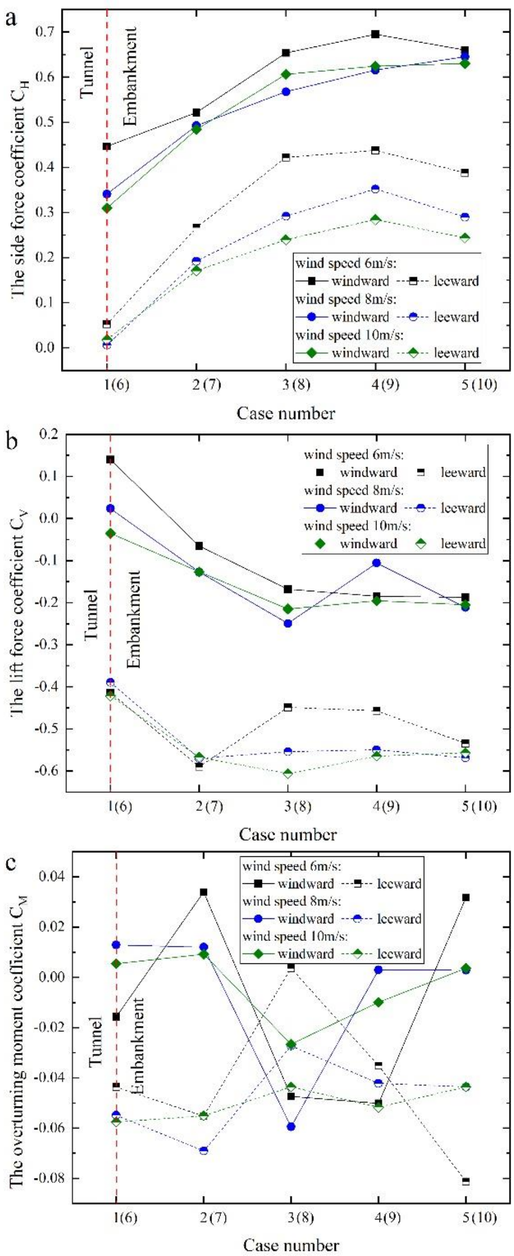

Fig. 13 Aerodynamic force coefficients at different positions along railway under the condition of single track

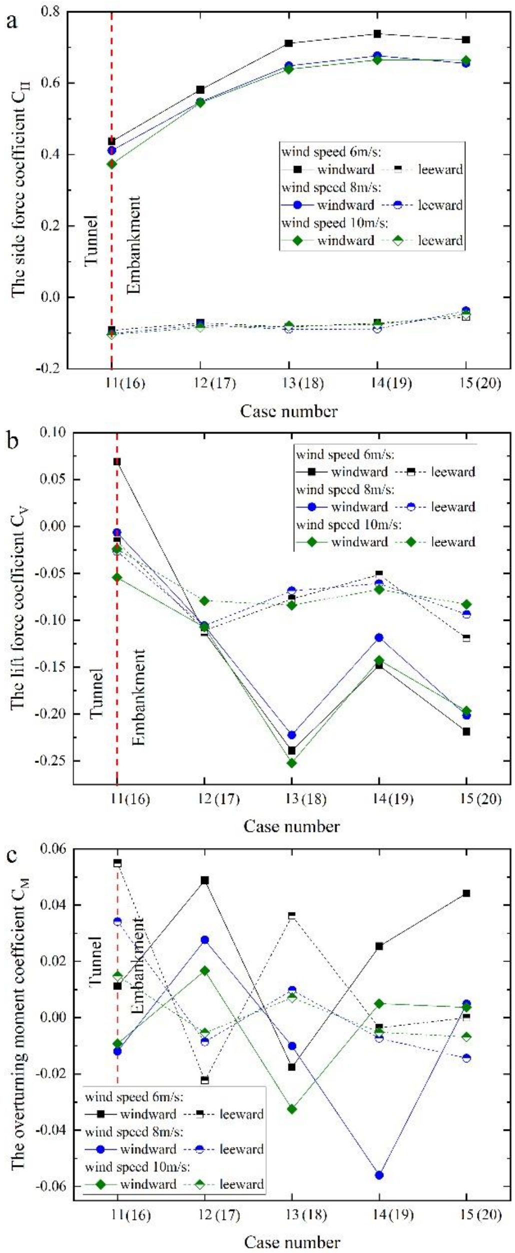

Fig. 14 Aerodynamic force coefficients at different positions along railway under the condition of double track

that when the vehicle is located at railway junction, the C_V of the vehicle on the windward side is positive. The positive status indicates that there is an upward force on the vehicle, which is biased to be unsafe. This may be caused by the flowing two factors: the first is near the railway junction, the airflow is compressed by the embankment, and the local compression increases the airflow speed, the second is that the embankment slope changes the airflow direction, and the oblique upward flow produces an oblique force on the vehicle. The weight of the intermediate vehicle is 3709 g, for the positive C_V cases, the ratios of the lift force to the weight of the vehicle are 2.1% (Case No.1, windward, 6 m/s) and 0.66% (Case No.1, windward, 8 m/s). Different from the windward side, the C_V on the leeward side is negative, and the downward force increases as the vehicle goes out of the tunnel. When the vehicle on the embankment, the absolute value of lift force on windward track is a bit larger than that on leeward track, but it's not agreed well in this tests due to the transition section (Cheli *et al*. 2010). Analyzing the data shown in Fig. 13(c), when the test vehicle goes out of the tunnel exactly (case 3 / 8), the C_M reaches the extremum. Comparing two tracks, the larger fluctuation makes the windward rail track more unfavorable.

(2) Interference between two trains

The relative results are shown in Fig. 14. As Fig. 14(a) shown, the C_H on the windward side is larger than that on the leeward side, this is because the windward side vehicle produces a significant shadowing effect on the leeward side vehicle. When the vehicle moving on the windward side, the C_H gradually increases as the vehicle moves out of the tunnel and tends to stabilize (cases 13 ~ 15 / cases 18 ~ 20). This is caused by the convex structure of the embankment and the locations of the vehicle. The embankment compresses the airflow and accelerates the flow speed, the vehicle windward area also increases when it goes out of the tunnel. When the vehicle is on the leeward side, the side force remains negative, because the windward rail track creates a shaded zone, the zone reduces the wind-induced force acting on the leeward side vehicle and creates negative pressure zone between two tracks so that the vehicle on leeward side suffers negative side force. Analyzing Fig. 14(b), the C_V of the vehicle on the windward side is similar with single track situation, the coefficient is negative except at the railway junction, and the value on the windward side is larger which means larger force. Same as single train case, the ratio of the lift force to the weight is 1% for Case No.11 when the wind speed is 6 m/s. As shown in Fig. 14(c), there is a greater correlation between overturning moment coefficient C_M and the side force coefficient C_V, the direction of the C_M on the windward and leeward sides is opposite. This can be explained that there is a higher speed vortex between two tracks, the vortex generates a lower pressure region and makes two tracks attracts each other. This explanation also provides the reason that the windward rail track C_H is positive while the leeward is negative.

4. Conclusions

In this paper, taking the subgrade-tunnel as the research object, which is divided into the cutting-tunnel transition section and the embankment-tunnel transition section. The variation of wind speeds at different positions of the transition section is studied, and the aerodynamic changes of the vehicle on the windward side and the leeward sides of the railway are discussed. Thus, the following conclusions are obtained:

(1) The influence range of cutting-tunnel transition section is larger than that of the embankment-tunnel transition section. The influence height of cutting-tunnel transition section is 320 mm (corresponding to 6.4 m in full scale), while the embankment-tunnel transition section is 240 mm (corresponding to 4.8 m in full scale).

(2) The wind speed profile at the line junction is greatly affected by the tunnel. Meanwhile, the contour and local enlargement of the tunnel portal has great influence.

(3) The side force coefficient on the windward side is basically larger than that on the leeward side. The value increases first and decreases in the case of the cutting-tunnel transition section, while increases first and then tends to be stable in the case of embankment-tunnel transition section. Compared with the single-track case, the coefficient under double track is larger, and the side force coefficient of the vehicle on the leeward side could be negative.

(4) When the vehicle passes through the embankment-tunnel transition section, the lift force coefficient could be positive which has adverse effects on the operation safety of the train.

For the actual high-speed railway projects, the wind barriers installed on the transition section may be a better choice to decrease the aerodynamic influence. In future, the wind tunnel tests for moving vehicle cases should be considered.

Acknowledgments

The work described in this paper was supported by grants from the Nation Natural Science Foundations of China (project nos. U1334201, 51525804 and 51708464). Also supported from the program for the Sichuan Province Youth Science and Technology Innovation Team (project no. 2015TD0004).

References

Alonso-Estébanez, A., Díaz, J.J.D.C., Rabanal, F.P.Á., Pascual-Muñoz, P. and Nieto, P.J.G. (2018), "Numerical investigation of truck aerodynamics on several classes of infrastructures", *Wind Struct*., **26**(1), 35-43.

Avila-Sanchez, S., Pindado, S., Lopez-Garcia, O. and Sanz-Andres, A. (2014), "Wind tunnel analysis of the aerodynamic loads on rolling stock over railway embankments: The effect of shelter windbreaks", *The Scientific World J*., **2014**, 17.

Baker, C., Cheli, F., Orellano, A., Paradot, N., Proppe, C. and Rocchi, D. (2009), "Cross-wind effects on road and rail vehicles", *Vehicle. Syst. Dyn.*, **47**(8), 983-1022.

Baker, C.J. (1985), "The determination of topographical exposure factors for railway embankments", *J. Wind Eng. Ind. Aerod.*, **21**(1), 89-99.

Baker, C.J., Jones, J., Lopez-Calleja, F. and Munday, J. (2004), "Measurements of the cross wind forces on trains", *J. Wind Eng. Ind. Aerod*., **92**(7), 547-563.

Bocciolone, M., Cheli, F., Corradi, R., Muggiasca, S. and Tomasini, G. (2008), "Crosswind action on rail vehicles: Wind tunnel experimental analyses", *J. Wind Eng. Ind. Aerod.*, **96**(5), 584-610.

Cheli, F., Corradi, R., Rocchi, D., Tomasini, G. and Maestrini, E. (2010), "Wind tunnel tests on train scale models to investigate the effect of infrastructure scenario", *J. Wind Eng. Ind. Aerod.*, **98**(6), 353-362.

Cheli, F., Giappino, S., Rosa, L., Tomasini, G. and Villani, M. (2013), "Experimental study on the aerodynamic forces on railway vehicles in presence of turbulence", *J. Wind Eng. Ind. Aerod*., **123**, 311-316.

Chen, S.R. and Cai, C.S. (2004), "Accident assessment of vehicles on long-span bridges in windy environments", *J. Wind Eng. Ind. Aerod*., **92**(12), 991-1024.

Diedrichs, B., Sima, M., Orellano, A. and Tengstrand, H. (2007), "Crosswind stability of a high-speed train on a high embankment", *Proc. Inst. Mech. Eng. Part F J. Rail Rapid Transit*., **221**(2), 205-225.

Dorigatti, F., Sterling, M., Baker, C.J. and Quinn, A.D. (2015), "Crosswind effects on the stability of a model passenger train – A comparison of static and moving experiments", *J. Wind Eng. Ind. Aerod*., **138**, 36-51.

Fujii, T., Maeda, T., Ishida, H., Imai, T., Tanemoto, K. and Suzuki, M. (1999), "Wind-induced accidents of train/vehicles and their measures in Japan", *Q. Rep. RTRI*., **40**(1), 50-55.

Ge, S.C. and Jiang, F.Q. (2009), “Analyses of the causes for wind disaster in strong wind area long Lanzhou-Xinjiang railway and the effect of windbreak”, *J. China Railw. Soc.*, **5**, 1-4. (in Chinese)

Giappino, S., Rocchi, D., Schito, P. and Tomasini, G. (2016), "Cross wind and rollover risk on lightweight railway vehicles", *J. Wind Eng. Ind. Aerod.*, **153**, 106-112.

He, X.H., Zou, Y.F., Wang, H.F., Han, Y. and Shi, K. (2014), “Aerodynamic characteristics of a trailing rail vehicles on viaduct based on still wind tunnel experiments”, *J. Wind Eng. Ind. Aerod.*, **135**, 22-33.

Hu, P. and Pan, X. (2010), “Embankment wind velocity field and traffic safety under the influence of sudden cross-wind”, *Proceedings of the 3rd IEEE International Conference on Science and Information Technology (ICCSIT)*, Beijing, China, July.

Kwon, H., Nam, S. and You, W. (2010), “Wind tunnel testing on crosswind aerodynamic forces acting on railway vehicles”, *J. Fluid Science Technol.*, **5**(1), 56-63.

Li, Y., Hu, P., Cai, C.S., Zhang, M. and Qiang, S. (2013), “Wind tunnel study of a sudden change of train wind loads due to the wind shielding effects of bridge towers and passing trains”, *J. Eng. Mech.*, **139**(9), 1249-1259.

Liu, T., Chen, Z., Zhou, X. and Zhang, J. (2018), “A CFD analysis of the aerodynamics of a high-speed train passing through a windbreak transition under crosswind”, *Eng. Appl. Comput. Fluid Mech.*, **12**(1), 137-151.

Quinn, A.D., Robertson, A.P., Hoxey, R.P., Short, J.L., Burgess, L.R. and Smith, B.W. (1998), “The effect of small embankments on wind speeds”, *Wind Struct*., **1**(4), 303-315.

Raghunathan, R.S., Kim, H.D. and Setoguchi, T. (2002), “Aerodynamics of high-speed railway train”, *Prog. Aeronaut. Sci.*, **38**(6), 469-514.

Schober, M., Weise, M., Orellano, A., Deeg, P. and Wetzel, W. (2010), “Wind tunnel investigation of an ICE 3 endcar on three standard ground scenarios”, *J. Wind Eng. Ind. Aerod.*, **98**(6), 345-352.

Suzuki, M., Tanemoto, K. and Maeda, T. (2003), “Aerodynamic characteristics of train/vehicles under cross winds”, *J. Wind Eng. Ind. Aerod.*, **91**(1), 209-218.

TB 10621-2014 (2014), Code for design for high speed railway, National Railway Administration of the People's Repulic of China, Beijing, China (in Chinese)

Tomasini, G., Giappino, S. and Corradi, R. (2014), “Experimental investigation of the effects of embankment scenario on railway vehicle aerodynamic coefficients”, *J. Wind Eng. Ind. Aerod.*, **131**, 59-71.

Xia, H., Guo, W.W., Zhang, N. and Sun, G.J. (2008), “Dynamic analysis of a train–bridge system under wind action”, *Comput. Struct.*, **86**(19), 1845-1855.

Xiong, X.H., Liang, X.F., Gao, G. and Liu, T.H. (2006), “Train aerodynamic characteristics in strong cross-wind on Lanzhou-Xinjiang railway line”, *J. Cent. South Univ.（Science Technol.）*, **37**, 1183-1188. (in Chinese)

Xu, Y.L., Xia, H. and Yan, Q.S. (2003), “Dynamic response of suspension bridge to high wind and running train”, *J. Bridge Eng.*, **8**(1), 46-55.

Zhang, J., Gao, G., Liu, T. and Li, Z. (2015), “Crosswind stability of high-speed trains in special cuts”, *J. Cent. South Univ.*, **22**(7), 2849-2856.

AD